Available online at www.sciencedirect.com
SCIENCE DIRECT®
International Journal of Heat and Mass Transfer 49 (2006) 3060–3067
International Journal of HEAT and MASS TRANSFER
www.elsevier.com/locate/ijhmt

# Thermally developing flow and heat transfer in rectangular microchannels of different aspect ratios

Poh-Seng Lee, Suresh V. Garimella *

*Cooling Technologies Research Center, School of Mechanical Engineering, Purdue University, West Lafayette, IN 47907-2088, USA*

Received 8 September 2005; received in revised form 3 February 2006
Available online 4 April 2006

**Abstract**

Laminar convective heat transfer in the entrance region of microchannels of rectangular cross-section is investigated under circumferentially uniform wall temperature and axially uniform wall heat flux thermal boundary conditions. Three-dimensional numerical simulations were performed for laminar thermally developing flow in microchannels of different aspect ratios. Based on the temperature and heat flux distributions obtained, both the local and average Nusselt numbers are presented graphically as a function of the dimensionless axial distance and channel aspect ratio. Generalized correlations, useful for the design and optimization of microchannel heat sinks and other microfluidic devices, are proposed for predicting Nusselt numbers. The proposed correlations are compared with other conventional correlations and with available experimental data, and show very good agreement.


*Keywords:* Microchannel; Thermally developing; Electronics cooling; Liquid cooling; Heat sink

## 1. Introduction

The increased power dissipation and shrinking dimensions of microelectronics devices have accentuated the need for highly effective compact cooling technologies. Microchannel heat sinks are of particular interest due to the very high rates of heat transfer they enable in conjunction with greatly reduced heat sink length scales and coolant mass. A significant amount of research has been dedicated to microchannel transport in recent years, as reviewed in [1,2]. Although, a number of published results on heat transfer in microchannels have differed from the behavior expected at "conventional," i.e., larger, length scales, recent work by Lee et al. [3] found that numerical predictions based on a classical, continuum approach are in good agreement with the experimental data when the entrance and boundary conditions imposed in the experiment are carefully matched in the simulation.

The unique characteristics of microchannel heat sinks (small length scales, conductive substrate, abrupt contraction/expansion at the entrance/exit, and high pressure drop) give rise to conditions that are quite different from those of conventional channels. For abrupt contraction/expansion at the entrance/exit, Rohsenow et al. [4] suggested that the inlet condition should be assumed as being hydrodynamically fully developed but thermally developing, due to wake effects at the abrupt entrance prior to the channel. Lee et al. [3] verified this using a computational analysis which included inlet and exit manifolds and concluded that flows in microchannel heat sinks typically experience thermally developing laminar flow, with significant entrance effects. It is important for the design of microchannel heat sinks to be able to accurately predict the heat transfer coefficients under different flow and thermal conditions, especially in developing laminar flow. In contrast to ducts with cross-sections defined by a single coordinate, such as circular tubes and parallel plates, where analytical solutions may be readily obtained, the analysis of heat transfer in a rectangular duct is more complicated

* Corresponding author. Tel.: +1 765 494 5621; fax: +1 765 494 0539.
*E-mail address:* sureshg@purdue.edu (S.V. Garimella).

0017-9310/$ - see front matter © 2006 Elsevier Ltd. All rights reserved.
doi:10.1016/j.ijheatmasstransfer.2006.02.011

**Nomenclature**

| | |
|---|---|
| $a$ | channel width, μm |
| $b$ | channel height, μm |
| $c_p$ | specific heat, kJ/kg °C |
| $D_h$ | hydraulic diameter, μm |
| $h$ | convective heat transfer coefficient, W/m$^2$ °C |
| $k$ | thermal conductivity, W/m °C |
| $l$ | channel length, mm |
| $\dot{m}$ | mass flow rate, kg/s |
| $n$ | index |
| $Nu$ | Nusselt number ($Nu = hD_h/k$) |
| $p$ | pressure, N/m$^2$ |
| $Pr$ | Prandtl number ($Pr = \mu c_p/k$) |
| $q''$ | heat flux, W/m$^2$ |
| $R^2$ | correlation coefficient |
| $Re$ | channel Reynolds Number ($Re = \rho u D_h/\mu$) |
| $T$ | temperature, °C |
| $u$ | velocity, m/s |
| $x$ | $x$-coordinate, mm |
| $y$ | $y$-coordinate, mm |
| $z$ | $z$-coordinate (axial distance), mm |
| $z_{th}$ | thermal entrance length, mm |
| $z^*$ | dimensionless axial distance ($z^* = z/ReD_hPr$) |
| $z^*_{th}$ | dimensionless thermal entrance length ($z^*_{th} = z_{th}/ReD_hPr$) |

*Greek symbols*

| | |
|---|---|
| $\alpha$ | channel aspect ratio ($\alpha = b/a$) |
| $\delta$ | thickness of the thin microchannel wall, μm |
| $\rho$ | density of water, kg/m$^3$ |
| $\mu$ | dynamic viscosity, Ns/m$^2$ |
| $\infty$ | fully developed |

*Subscripts*

| | |
|---|---|
| ave | average |
| f | fluid |
| fd | fully developed flow |
| m | mean |
| z | local |
| w | wall |

and most studies have employed numerical approaches [5,6].

Accurate prediction of heat transfer coefficients also requires the correct thermal boundary conditions to be faithfully simulated. In applications where microchannel heat sinks are used, a uniform heat flux is usually applied to the base of the heat sink substrate, which is often made of a conductive material such as silicon, copper or aluminum to reduce overall thermal resistances. Three-dimensional conjugate heat transfer thus takes place within the heat sink, leading to the redistribution of heat flux and temperature along the channel walls. Though three-dimensional conjugate heat transfer analyses have been shown to provide satisfactory simulations of experimental conditions [3,7], they are computationally expensive and case-specific, and cannot be generalized to a wide range of microchannel configurations. To simplify the full three-dimensional conjugate analysis, the computational domain has typically been restricted to include only the fluid region, with one of the following alternative thermal boundary conditions applied to the channel walls: H1 (circumferentially constant wall temperature and axially constant wall heat flux), H2 (uniform wall heat flux, both axially and circumferentially), and $T$ (uniform wall temperature, both axially and circumferentially) [8]. While all the details of the actual thermal problem are not faithfully represented by means of these simplifications, such approaches are more computationally economical since conduction in the substrate is not included in the calculation procedure. Importantly, the results of such analyses can be generalized to microchannels of different dimensions, de-coupled from details of the substrate.

Lee et al. [3] conducted a detailed, three-dimensional conjugate heat transfer analysis for the copper microchannel heat sink used in their work (with a uniform heat flux imposed on the bottom wall of the substrate). They compared the results from their analysis to those obtained from simplified analyses for a microchannel using the H1, H2 and $T$ boundary conditions on the channel wall. With the three-dimensional conjugate heat transfer model, a computational grid of $50 \times 160 \times 100$ cells had to be used, whereas for the simplified analyses only an eighth of the grid size ($20 \times 50 \times 100$ cells) was required. Predictions from the H1 thermal boundary condition were found to be in the best agreement with the full three-dimensional conjugate analysis, deviating by less than 1.3%. They concluded that the H1 thermal boundary condition is the most appropriate for simplified analyses, when full conjugate analyses are not affordable. The H1 thermal boundary condition is common in engineering problems such as electric resistance heating, nuclear heating, counterflow heat exchangers having nearly identical fluid capacity rates, all with highly conductive wall materials [9].

Wibulswas [5] solved the thermal entrance length problem with the H1 boundary condition; fluid axial conduction and viscous dissipation were neglected and it was assumed that no heat sources were present in the domain. Aparecido and Cotta [6] solved the problem of thermally developing flow in square ducts for the $T$ boundary condition. However, both these sets of results were limited to a small range of channel aspect ratios ($\alpha = 1$–4), and were also restricted by the available computational resources of the time. With the increased power of the modern computer, much improved computational fluid dynamics

(CFD) computations can be performed with high accuracy and flexibility.

In the present work, laminar flow and heat transfer in the thermal entrance region of rectangular ducts with aspect ratios ranging from 1 to 10 is investigated for thermally developing flow with the H1 thermal boundary condition. A finite volume approach is employed to obtain the temperature and heat flux distributions on the channel walls. The local and average Nusselt numbers in the entrance region are numerically calculated as functions of the dimensionless axial distance and channel aspect ratio. Generalized correlations for both the local and average Nusselt numbers in the thermal entrance region are proposed. The results are compared to predictions from correlations for conventional channels as well as with experimental data for microchannels, and good agreement is noted. The proposed correlations are easy to use, provide detailed heat transfer coefficient predictions in the entrance region of microchannels, and cover a wide parameter range.

## 2. Mathematical formulation

The following assumptions are made to model the heat transfer in the rectangular channel:

(1) steady state,
(2) incompressible fluid,
(3) laminar flow,
(4) constant fluid properties,
(5) negligible axial conduction and viscous dissipation, and
(6) negligible radiative and natural convective heat transfer from the microchannel heat sink.

The dimensions of the microchannels considered in this work are listed in Table 1. To achieve the H1 boundary condition, a very thin and highly conductive wall (but with no axial conduction) is included in the model. The width ($a$) and axial length ($l$) of the channel in the computational model are held constant at 200 μm and 120 mm, respectively, while the height ($b$) of the channel is varied. The aspect ratio of the rectangular channel and its hydraulic diameter are defined as

$$\alpha = \frac{b}{a} \quad \text{and} \quad D_h = \frac{2ab}{a+b} \tag{1}$$

Fig. 1 shows a schematic diagram of the microchannel cross-section considered. Only a quarter of the microchannel was included in the computational domain, in view of the symmetry conditions.

The governing equations for mass, momentum and energy are solved with boundary conditions as follows. The velocity is zero on all wall boundaries, and as the flow is assumed to be hydrodynamically fully developed, the following exact analytical solution by Marco and Han [10] is used as the fully developed inlet velocity profile:

$$\left.\begin{aligned} u(x,y,0) &= -\frac{16}{\pi^3}\left(\frac{dp}{dz}\right)\frac{(b/2)^2}{\mu} \\ &\quad \times \sum_{n=1,3,\ldots}^{\infty} \frac{(-1)^{(n-1)/2}}{n^3}\left(1-\frac{\cosh(n\pi y/b)}{\cosh(n\pi a/2b)}\right)\cos\left(\frac{n\pi x}{b}\right) \\ v(x,y,0) &= 0 \\ w(x,y,0) &= 0 \end{aligned}\right\} \tag{2}$$

where the pressure gradient $dp/dz$ is given in terms of the mean fluid velocity, $u_m$, by

$$u_m = -\frac{1}{3}\left(\frac{dp}{dz}\right)\frac{(b/2)^2}{\mu}\left[1-\frac{192}{\pi^5}\left(\frac{b}{a}\right)\sum_{n=1,3,\ldots}^{\infty}\frac{1}{n^5}\tanh\left(\frac{n\pi a}{2b}\right)\right] \tag{3}$$

An outflow boundary condition is specified at the channel outlet. A uniform heat flux is applied to all the external boundaries of the thin wall region while the liquid at the inlet is given a uniform temperature profile.

Table 1
Dimensions of the microchannels investigated

| α | $a$ (μm) | $b$ (μm) | $D_h$ (μm) | $L$ (mm) | Mesh (quarter domain) |
|---|---|---|---|---|---|
| 1 | 200 | 200 | 200 | 120 | 10 × 10 × 400 |
| 2 | 200 | 400 | 267 | 120 | 10 × 20 × 400 |
| 3 | 200 | 600 | 300 | 120 | 10 × 30 × 400 |
| 4 | 200 | 800 | 320 | 120 | 10 × 40 × 400 |
| 5 | 200 | 1000 | 333 | 120 | 10 × 50 × 400 |
| 6 | 200 | 1200 | 343 | 120 | 10 × 60 × 400 |
| 7 | 200 | 1400 | 350 | 120 | 10 × 70 × 400 |
| 8 | 200 | 1600 | 356 | 120 | 10 × 80 × 400 |
| 9 | 200 | 1800 | 360 | 120 | 10 × 90 × 400 |
| 10 | 200 | 2000 | 364 | 120 | 10 × 100 × 400 |

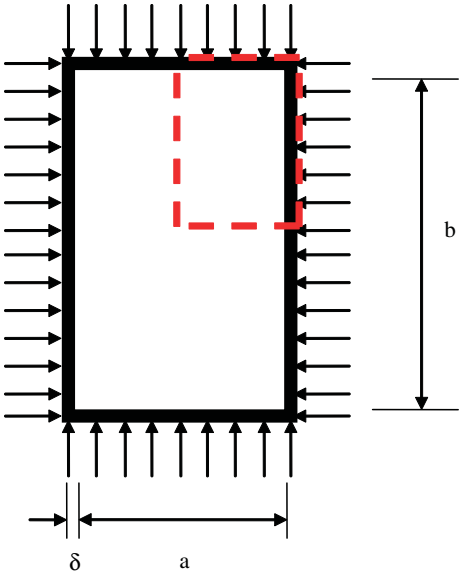


Fig. 1. Microchannel with thin conductive wall. The computational domain chosen from symmetry conditions is indicated with dashed lines.

Symmetry boundaries are used to reduce the extent of the computational model to a symmetric quarter-domain. There is no convective flux across a symmetry plane, so that the normal velocity component at the symmetry plane is thus zero. There is also no diffusion flux across the symmetry plane, rendering the normal gradients of all flow variables to be zero at the symmetry plane.

### 2.1. Solution method

The continuity equation and the Navier–Stokes equations in their steady, incompressible form, along with the associated boundary conditions were solved using the general-purpose finite-volume based computational fluid dynamics (CFD) software package, FLUENT [11]. An axially constant wall heat flux of 50 W/cm$^2$ with circumferentially constant wall temperature, i.e., the H1 thermal boundary condition, was applied on all four walls. This boundary condition has been shown by Lee et al. [3] to closely approximate the full three-dimensional conjugate heat transfer analysis with uniform heat flux applied to the bottom of the substrate as typically encountered in power electronics. Water enters the microchannels with a fully developed velocity profile at a temperature of 300 K. Only flow rates in the laminar regime were considered. The standard scheme was used for pressure discretization. The SIMPLE algorithm was employed for velocity–pressure coupling in the multi-grid solution procedure. The momentum and energy equations were solved with a first-order upwind scheme.

The entire domain was meshed using hexahedral elements. For the microchannel with aspect ratio of five, for example, a computational grid of $10 \times 50 \times 400$ cells (for quarter channel) was used. The channel width and height were meshed with a uniform grid while the channel length was meshed with a double successive ratio of 1.02. The meshes used for the different aspect ratios are included in Table 1.

The local heat flux and local temperature distributions are obtained from the numerical simulations. With these quantities, the local convective heat transfer coefficient, $h(z)$, can be evaluated using the following equation:

$$h(z) = \frac{1}{A(z)} \frac{q(z)}{\sum_{x,y}[T_w(x,y,z) - T_m(z)]\mathrm{d}A(x,y,z)} \tag{4}$$

where $A(z)$ and $q(z)$ are the total local heat transfer area and total local heat input, respectively, as defined below

$$A(z) = \sum_{x,y} \mathrm{d}A(x,y,z) \tag{5}$$

$$q(z) = \sum_{x,y} q''(x,y,z)\mathrm{d}A(x,y,z) \tag{6}$$

In Eq. (4), $T_w(x,y,z)$ is the local wall temperature and $T_m(z)$ is local fluid bulk-mean temperature given by

$$T_m(z) = T_{in} + \frac{1}{\dot{m}C_p} \sum_{x,y,z} q''(x,y,z)\mathrm{d}A(x,y,z) \tag{7}$$

The local Nusselt number, $Nu(z)$, can then be calculated using

$$Nu(z) = \frac{D_h}{k_f} \times h(z) \tag{8}$$

The average Nusselt number, $Nu_{ave}(z)$, can similarly be computed as

$$Nu_{ave}(z) = \frac{D_h}{k_f} \times \frac{1}{\sum_{x,y,z}\mathrm{d}A(x,y,z)} \times \frac{\sum_{x,y,z} q''(x,y,z)\mathrm{d}A(x,y,z)}{\sum_{x,y,z}[T_w(x,y,z) - T_m(z)]\mathrm{d}A(x,y,z)} \tag{9}$$

### 2.2. Grid-independence

The meshes tabulated in Table 1 for the different channel aspect ratios were verified to result in grid-independent results. As an example, local Nusselt numbers of 6.21, 6.15, and 6.11 were obtained for a channel aspect ratio of 5 with mesh sizes of $5 \times 25 \times 200$, $10 \times 50 \times 400$ and $15 \times 75 \times 600$, respectively, at $z = 60$ mm when $Re = 1100$. The local Nusselt number changed by 1.7% from the first to the second mesh, and only by 0.7% upon further refinement to the finest grid. Hence the intermediate $(10 \times 50 \times 400)$ grid was chosen. This grid-independence is also illustrated graphically in Fig. 2. Grid-independence was similarly established for the meshes selected for the other channel aspect ratios.

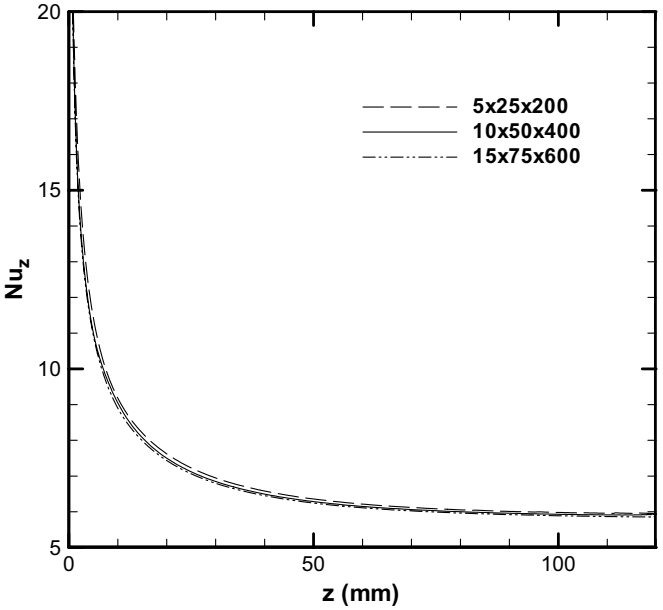


Fig. 2. Variation of local Nusselt number with axial distance for each of the different grids considered.

## 3. Results and discussion

### 3.1. Local and average Nusselt numbers

Fig. 3 shows the local Nusselt number as a function of dimensionless axial distance, $z^* = z/(Re\,Pr\,D_h)$ and aspect ratio ($\alpha$). As expected due to the growth of the thermal boundary layer, the Nusselt number is very high at the beginning of the entrance region, but rapidly decreases and asymptotically approaches the fully developed values, given by the formula [8],

$$Nu_\infty = 8.235\left(1 - \frac{2.0421}{\alpha} + \frac{3.0853}{\alpha^2} - \frac{2.4765}{\alpha^3} + \frac{1.0578}{\alpha^4} - \frac{0.1861}{\alpha^5}\right) \tag{10}$$

An interesting feature characteristic of rectangular channels is that the local heat-transfer conductance varies around the periphery and approaches zero at the square corners. This implies that the heat flux goes to zero at the corners [12]. Svino and Siegel [13] investigated the effect of unequal heat addition on adjacent sides of rectangular channels and found that poor convection due to low velocities in the corners and along the narrow wall causes peak temperatures to occur at the corners. Also, lower peak temperatures occur when only the longer sides are heated. This is reflected in the increase in local Nusselt number in the microchannel at a larger aspect ratio, since the relative importance of the narrow walls and corners diminishes with increasing aspect ratio.

The dimensionless thermal entrance length, $z^*_{th}$, defined as the distance required over which the local Nusselt number, $Nu_z$, drops to 1.05 times the fully developed value, $Nu_\infty$, can be determined from the results. Fig. 4 shows these values as a function of the channel aspect ratio. A larger aspect ratio channel is observed to have a shorter dimensionless thermal entrance length. The following relationship was curve-fit to the results with a correlation coefficient ($R^2$) of 1:

$$z^*_{th} = -1.275\times10^{-6}\alpha^6 + 4.709\times10^{-5}\alpha^5 - 6.902\times10^{-4}\alpha^4 + 5.014\times10^{-3}\alpha^3 - 1.769\times10^{-2}\alpha^2 + 1.845\times10^{-2}\alpha + 5.691\times10^{-2} \tag{11}$$

This correlation can be used to demarcate the developing regime from the fully developed regime. For accurate prediction of the heat transfer performance of a microchannel heat sink, the entrance effects need to be taken into account in the developing section, beyond which, the fully developed analysis is valid.

The average Nusselt number is shown in Fig. 5 as a function of dimensionless axial distance and aspect ratio. As in the case of the local Nusselt number, the average value starts high and decreases rapidly with downstream distance.

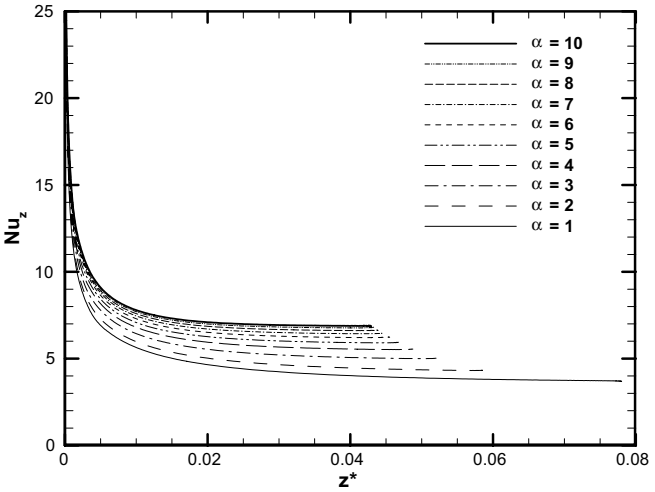


Fig. 3. Local Nusselt number as a function of dimensionless length and aspect ratio.

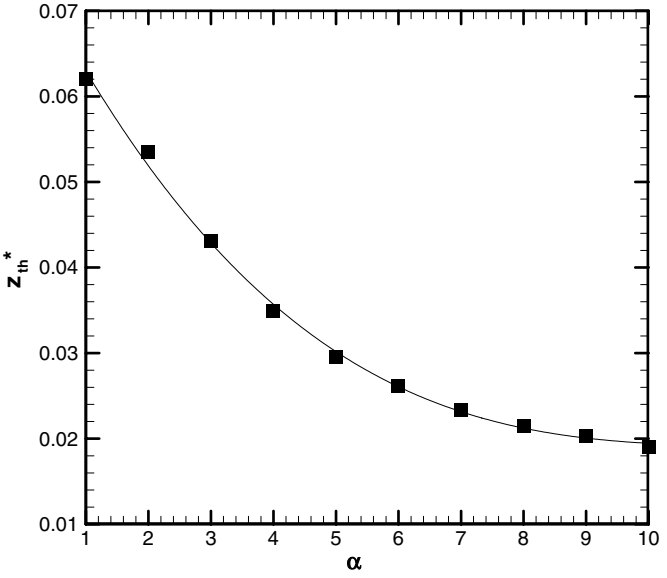


Fig. 4. Dimensionless thermal entrance length as a function of the channel aspect ratio. The curve-fit in the plot represents Eq. (11).

### 3.2. Nusselt number correlations

The following generalized correlation for local Nusselt number was obtained as a function of axial distance and channel aspect ratio from a regression analysis with a residual tolerance of $1\times10^{-10}$ applied to 4000 computed values:

$$Nu_z = \frac{1}{C_1(z^*)^{C_2} + C_3} + C_4, \quad \text{for } 1 \leqslant \alpha \leqslant 10,\ z^* < z^*_{th} \tag{12}$$

in which

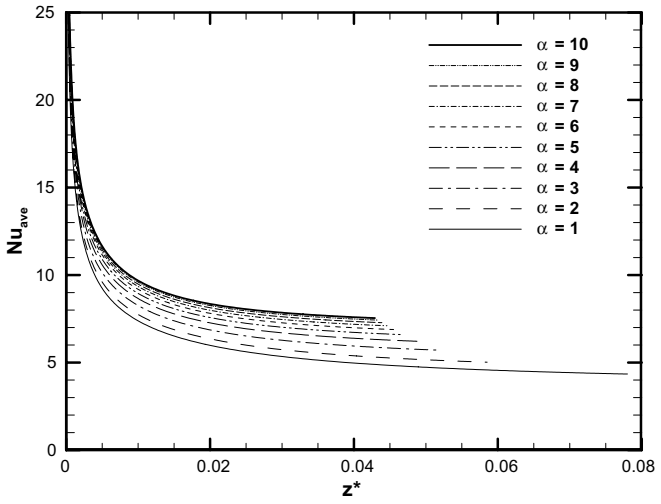


Fig. 5. Average Nusselt number as a function of dimensionless length and aspect ratio.

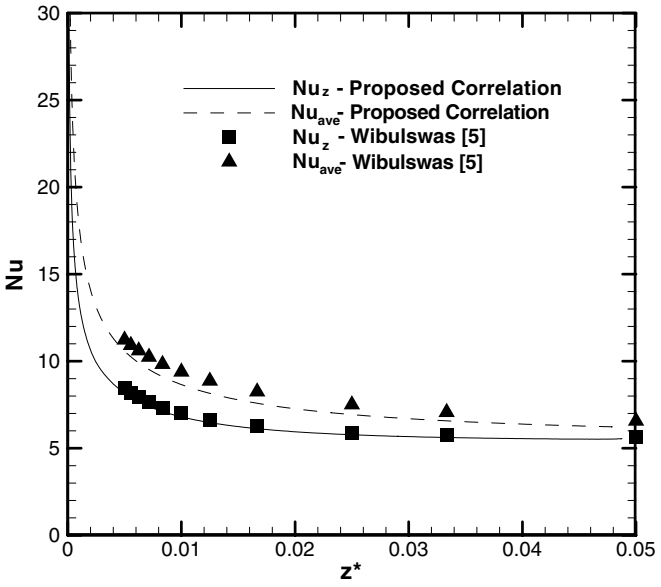


Fig. 6. Comparison of present work with that of Wibulswas [5] for $\alpha = 4$.

$$C_1 = -3.122\times10^{-3}\alpha^3 + 2.435\times10^{-2}\alpha^2 + 2.143\times10^{-1}\alpha + 7.325$$
$$C_2 = 6.412\times10^{-1}$$
$$C_3 = 1.589\times10^{-4}\alpha^2 - 2.603\times10^{-3}\alpha + 2.444\times10^{-2}, \text{ and}$$
$$C_4 = 7.148 - 1.328\times10^{1}/\alpha + 1.515\times10^{1}/\alpha^2 - 5.936/\alpha^3$$

The fitted correlation has a very small average residual of $2.697\times10^{-13}$ and an excellent correlation coefficient ($R^2$) of 0.999. This correlation is applicable when the flow is thermally developing, i.e., when $z^* < z^*_{\text{th}}$ from Eq. (11). Beyond $z^*_{\text{th}}$, the flow can be assumed to be fully developed, and Eq. (10) should be used instead.

A generalized correlation of very similar form was obtained for the average Nusselt number as well:

$$Nu_{\text{ave}} = \frac{1}{C_1(x^*)^{C_2} + C_3} + C_4, \quad \text{for } 1 \leqslant \alpha \leqslant 10,\ z^* < z^*_{\text{th}} \tag{13}$$

where

$$C_1 = -2.757\times10^{-3}\alpha^3 + 3.274\times10^{-2}\alpha^2 - 7.464\times10^{-5}\alpha + 4.476$$
$$C_2 = 6.391\times10^{-1}$$
$$C_3 = 1.604\times10^{-4}\alpha^2 - 2.622\times10^{-3}\alpha + 2.568\times10^{-2}, \text{ and}$$
$$C_4 = 7.301 - 1.311\times10^{1}/\alpha + 1.519\times10^{1}/\alpha^2 - 6.094/\alpha^3$$

The fitted correlation again has a very small average residual of $-9.684\times10^{-13}$ and an excellent correlation coefficient ($R^2$) of 0.999.

### 3.3. Comparison with existing results for conventional channels

The numerical work of Wibulswas [5] perhaps most closely resembles the geometry (rectangular cross-section) and nature of the flow (thermally developing, with H1 boundary condition) considered in the present study. Predictions from the correlations proposed based on the results from the present study are compared to those of Wibulswas in Fig. 6, for a channel aspect ratio of four. While the agreement is, in general, quite good, the deviations between the two sets of results may be attributed to the very coarse mesh used in [5]. Also, Wibulswas reported very few data points near the channel entrance. In addition, the present work considers a much wider range of channel aspect ratios, and presents generalized correlations unlike the limited data available in [5].

Perkins et al. [14] proposed the following correlation based on their experimental measurements of local Nusselt number for a square duct:

$$Nu_z = [0.277 - 0.152\exp(-38.6z^*)]^{-1} \tag{14}$$

The proposed correlations from the present study agree well with predictions from Eq. (14), as shown in Fig. 7, except in the region close to the channel inlet. Experimental data in this region were sparse, and therefore, the deviation in this region is not surprising.

Chandrupatla and Sastri [15] numerically analyzed the thermal entrance length problem for a square duct with the H1, H2 and $T$ boundary conditions. While they used finer grids than those of Wibulswas [5], and their results agree closely with the proposed correlation as shown in Fig. 7, limited data were reported in the region close to the channel entrance. Lee et al. [3] deduced the dimensionless entrance lengths in past experimental studies on microchannel heat sinks and observed that the majority of these studies encounter thermally developing state ($0.003 \leqslant z^* \leqslant 0.056$). As such, resolving the heat transfer in the entrance region is very important for the accurate prediction of microchannel heat sink performance.

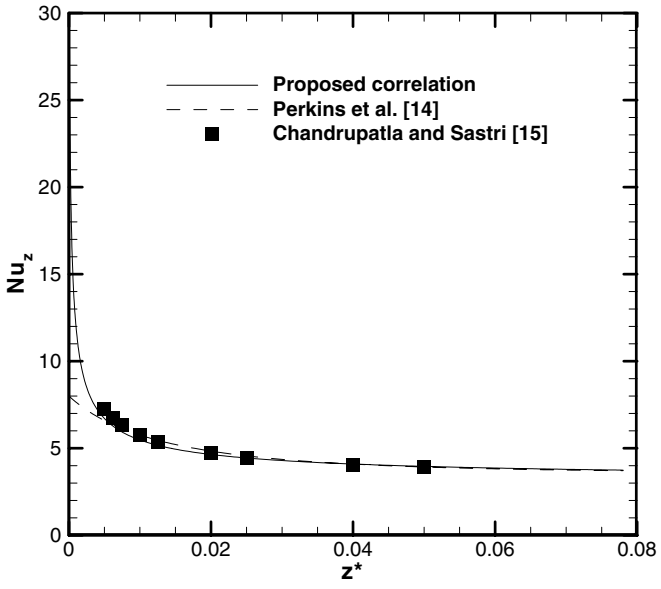


Fig. 7. Comparison of present work with that of Perkins et al. [14] and Chandrupatla and Sastri [15] for $\alpha = 1$.

It may be noted that the large aspect ratio ($\alpha > 4$) channels considered in this study are desirable due to the improvement in heat transfer coefficient with increasing aspect ratio. These deeper channels are readily fabricated by deep reactive ion etching (DRIE). Very limited information was available for the larger aspect ratios in the literature, and the correlations proposed here are important for the design and optimization of microchannel heat sinks.

### 3.4. Comparison with experimental data for microchannels

The proposed correlation for average Nusselt number was compared against experimental results obtained for microchannels in [3]. The experiments undertook a systematic investigation of single-phase laminar heat transfer in rectangular microchannels of widths ranging from 194 to 534 μm, with the channel depth being nominally five times the width. The test pieces were made of copper, and deionized water was used as the working fluid. In the experiments, only three walls were heated, with the top wall being made of an insulating material. The results from

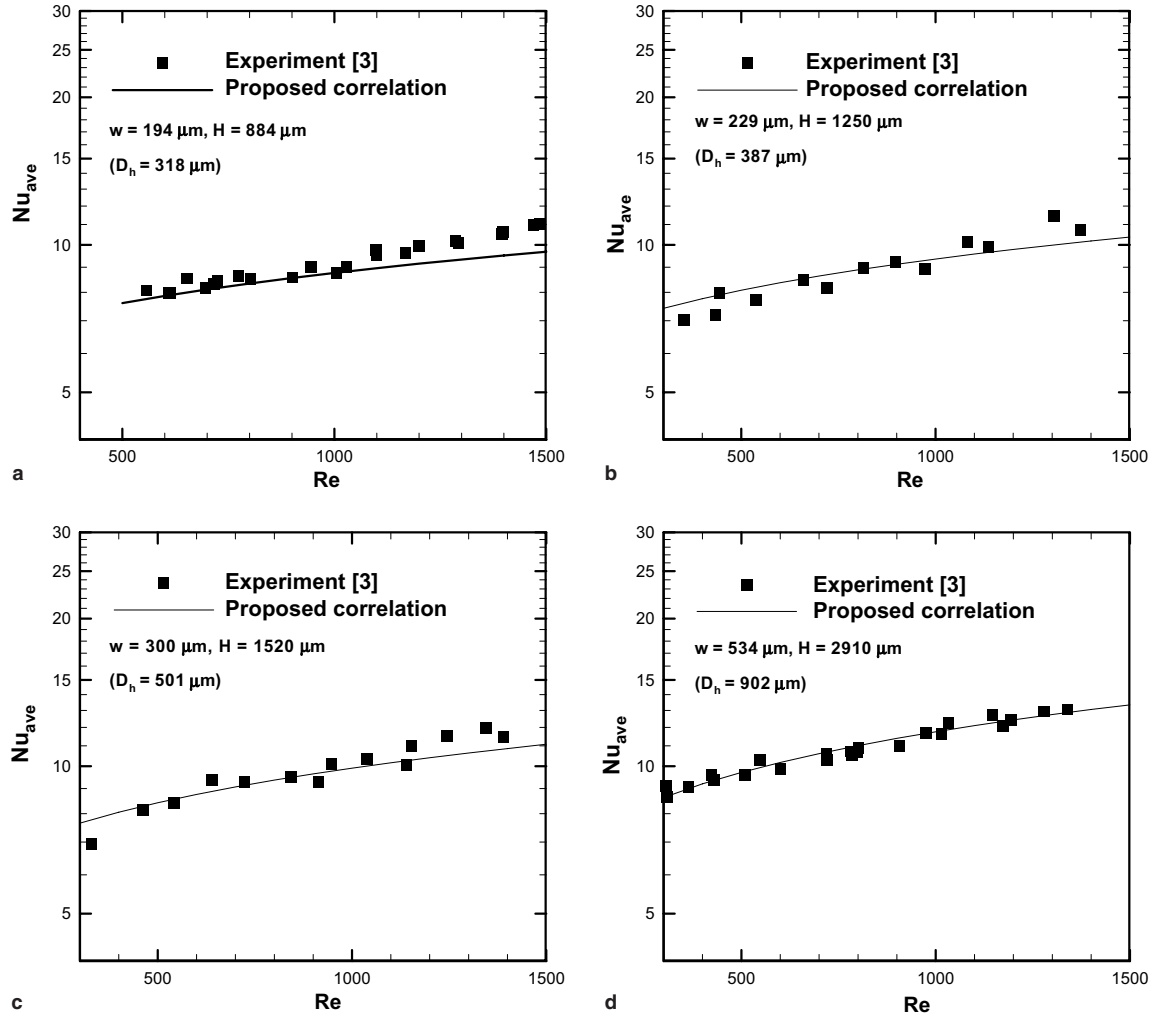


Fig. 8. Comparison of proposed correlation with experimental results of Lee et al. [3].

the present work, which considers heat transfer from all four sides of the rectangular channels, were adapted for comparison with the experiments using the correction factor proposed by Phillips [16]:

$$Nu_{z,3} = Nu_z \times (Nu_{\infty,3}/Nu_\infty) \tag{15}$$

This equation assumes that the ratio of developing Nusselt numbers for the three- and four-sided heating cases is identical to the value in fully developed flow. The fully developed Nusselt number for four-sided heating is given in Eq. (10) while that for the three-sided heating case can be approximated by the following formula [8]:

$$Nu_{\infty,3} = 8.235\left(1 - \frac{1.883}{\alpha} + \frac{3.767}{\alpha^2} - \frac{5.814}{\alpha^3} + \frac{5.361}{\alpha^4} - \frac{2.0}{\alpha^5}\right) \tag{16}$$

Fig. 8 shows the comparison for four different sets of experiments with microchannels of different dimensions. The agreement is very satisfactory, suggesting that the proposed correlations based on a classical, continuum approach may be employed in predicting heat transfer coefficients in microchannel heat sinks.

The development of these generalized Nusselt number correlations could significantly aid in the design of microchannel heat sinks as this allows accurate predictions of their thermal performance without the need for full three-dimensional conjugate heat transfer analyses.

## 4. Conclusions

Local and average Nusselt numbers in the laminar flow of a Newtonian fluid through rectangular microchannels is investigated. Microchannel heat sinks are found to be best represented by the so-called H1 thermal boundary condition. Numerical simulations based on the finite volume method were conducted to predict steady, laminar heat transfer coefficients in hydrodynamically developed but thermally developing flow. Generalized correlations for both the local and average Nusselt numbers in the thermal entrance region are proposed. Predictions from these correlations compare very favorably with previous computational and experimental results for conventional channels, as well as with experimental results for microchannel heat sinks. The proposed correlations allow accurate predictions of the thermal performance of microchannel heat sinks.

## Acknowledgements

The authors acknowledge the financial support from members of the Cooling Technologies Research Center, a National Science Foundation Industry/University Cooperative Research Center at Purdue University. Professor Jayathi Murthy is thanked for helpful discussions.

## References

[1] C.B. Sobhan, S.V. Garimella, A comparative analysis of studies on heat transfer and fluid flow in microchannels, Microscale Thermophys. Eng. 5 (2001) 293–311.
[2] S.V. Garimella, C.B. Sobhan, Transport in microchannels – A critical review, Annu. Rev. Heat Transfer 13 (2003) 1–50.
[3] P.S. Lee, S.V. Garimella, D. Liu, Investigation of heat transfer in rectangular microchannels, Int. J. Heat Mass Transfer 48 (2005) 1688–1704.
[4] W.M. Rohsenow, J.P. Hartnett, E.N. Ganic, Handbook of Heat Transfer Applications, McGraw-Hill, New York, 1985.
[5] P. Wibulswas, Laminar-flow heat-transfer in non-circular ducts, PhD thesis, University of London, 1966.
[6] J.B. Aparecido, R.M. Cotta, Thermally developing laminar flow inside rectangular ducts, Int. J. Heat Mass Transfer 33 (1990) 341–347.
[7] W. Qu, I. Mudawar, Experimental and numerical study of pressure drop and heat transfer in a single-phase micro-channel heat sink, Int. J. Heat Mass Transfer 45 (2002) 2549–2565.
[8] R.K. Shah, A.L. London, Laminar flow forced convection in ducts, Adv. Heat Transfer (Suppl. I) (1978).
[9] S. Kakac, R.K. Shah, W. Aung, Handbook of Single-Phase Convective Heat Transfer, 1987.
[10] S.M. Marco, L.S. Han, A note on limiting laminar Nusselt number in ducts with constant temperature gradient by analogy to thin-plate theory, Trans. ASME 77 (1995) 625–630.
[11] FLUENT 6 User's Guide, Lebanon, NH, Fluent Inc., 2000.
[12] W.M. Kays, M.E. Crawford, Convective Heat and Mass Transfer, third ed., 1993, pp. 125.
[13] J.M. Svino, R. Siegel, Laminar forced convection in rectangular channels with unequal heat addition on adjacent sides, Int. J. Heat Mass Transfer 16 (1964) 733–741.
[14] K.R. Perkins, K.W. Shade, D.M. McEligot, Heated laminarizing gas flow in a square duct, Int. J. Heat Mass Transfer 16 (1973) 897–916.
[15] A.R. Chandrupatla, V.M.L. Sastri, Laminar forced convection heat transfer of a non-Newtonian fluid in a square duct, Int. J. Heat Mass Transfer 20 (1977) 1315–1324.
[16] R.J. Phillips, Microchannel Heat Sinks, PhD thesis, Massachusetts Institute of Technology, 1987.